Arrangement of sympathetic fibers within the human common peroneal nerve: Implications for microneurography

Rebecca P.R. Tompkins
Schulich School of Medicine & Dentistry

C. W.J. Melling
Western University

Timothy D. Wilson
Western University

Brent D. Bates
Western University

J. Kevin Shoemaker
Western University, kshoemak@uwo.ca

Citation of this paper:

Tompkins, Rebecca P.R.; Melling, C. W.J.; Wilson, Timothy D.; Bates, Brent D.; and Shoemaker, J. Kevin, "Arrangement of sympathetic fibers within the human common peroneal nerve: Implications for microneurography" (2013). *Paediatrics Publications*. 1571.
https://ir.lib.uwo.ca/paedpub/1571

Arrangement of sympathetic fibers within the human common peroneal nerve: implications for microneurography

Rebecca P. R. Tompkins,[1,3] C. W. J. Melling,[2] Timothy D. Wilson,[3] Brent D. Bates,[2] and J. Kevin Shoemaker[2,4]

[1]*Department of Anatomy and Cell Biology, Schulich School of Medicine and Dentistry, University of Western Ontario, London, Ontario, Canada;* [2]*Faculty of Health Sciences, School of Kinesiology, University of Western Ontario, London, Ontario, Canada;* [3]*Corps for Research in Instructional and Perceptual Technologies, Department of Anatomy and Cell Biology, University of Western Ontario, London, Ontario, Canada; and* [4]*Department of Physiology and Pharmacology, Schulich School of Medicine and Dentistry, University of Western Ontario, London, Ontario, Canada*

Tompkins RP, Melling CWJ, Wilson TD, Bates BD, Shoemaker JK. Arrangement of sympathetic fibers within the human common peroneal nerve: implications for microneurography. *J Appl Physiol* 115: 1553–1561, 2013. First published October 3, 2013; doi:10.1152/japplphysiol.00273.2013.—Recently, interest has grown in the firing patterns of individual or multiunit action potential firing patterns in human muscle sympathetic nerve recordings using microneurography. Little is known, however, about sympathetic fiber distribution in human lower limb nerves that will affect the multiunit recordings. Therefore, the purpose of this study was to examine the sympathetic fiber distribution within the human common peroneal nerve using immunohistochemical techniques (tyrosine hydroxylase, avidin-biotin complex technique). Five-micrometer transverse and 10-μm longitudinal sections, fixed in formaldehyde, were obtained from the peroneal nerve that had been harvested from three human cadavers (83 ± 11 yr) within 24 h of death. Samples of rat adrenal gland and brain served as controls. Sympathetic fiber arrangement varied between left and right nerves of the same donor, and between donors. However, in general, sympathetic fibers were dispersed throughout ~25–38 fascicles of the peroneal nerve. The fibers were grouped in bundles of ~2–44 axons or expressed individually throughout the fascicles, and the distribution was skewed toward smaller bundles with median and interquartile ratio values of 5 and 1 axons/bundle, respectively. These findings confirm the bundled organization of sympathetic axons within the peroneal nerve and provide the anatomical basis for outcomes in microneurographic studies.

sympathetic axons; human; C fibers

SINCE THE FIRST NEURAL RECORDINGS of efferent sympathetic nerve activity by Hagbarth and Vallbo in 1968 (10), there has been growing interest in the patterned nature of the neural outflow and its implications for understanding the neurophysiological principles determining sympathetic discharge and the end organ response. A major limitation in such deliberations has been uncertainty regarding the anatomical bases of the axons from which the neural signal arises and the physical relationship between the microelectrode used in microneurography and these axons. Microneurographic measures of postganglionic sympathetic C-fiber activity in human peripheral nerves suggest that these axons must be grouped in a manner that can be impaled by the microelectrode, enabling recordings of multiunit sympathetic nerve activity. The anecdotal experience of microneurography indicates that these bundles must be rather small in both size and number of axons, as well as disparate, often requiring persistence on the part of the microneurographer to locate such a bundle and optimally locate the electrode within the corresponding axons.

Recently, signal processing techniques have been adapted to expose the location and timing of action potentials within each sympathetic burst and their discharge patterns (6, 23, 29). The results from our laboratory suggest that the number of action potentials per burst can range from 3 to 40 within the same electrode position (25, 28). These studies also indicated that axons of various sizes and conduction velocities must exist within these bundles. Previously, Macefield et al. (16) introduced the study of, and fundamental firing patterns of, single axons in young healthy humans, indicating that these axons generally fire one to two times during a burst. Neither of these approaches establishes the total number of axons available for recruitment, but they may provide predictive evidence that the minimal bundle size would be >1 axon and a theoretical maximum of ~40 axons.

Very little information exists regarding sympathetic C-fiber distribution in the peripheral nerves of humans, and existing data lead to varying conclusions. Using avidin-biotin complex (ABC) immunohistochemical methods, Marx and colleagues (17–19, 21) examined tyrosine hydroxylase (TH) expression in the human radial and antebrachial nerves as the marker of sympathetic axon anatomy. Their results indicated TH expression varied across branching levels of the radial nerve, and, instead of a bundled pattern, they observed a diffuse distribution of discreet TH-containing axons. However, the presence of what appears to be nonspecific binding of surrounding tissues, and the lack of bundling of axons, raises concerns regarding the relationship between the staining patterns and TH expression. Recently, the extensive innervation of the foot by sural nerve sympathetic neurons was demonstrated (5), but the bundled pattern of axons was not addressed in this nerve. In contrast, Balogh and colleagues (1) used similar methods to study TH-containing axons in the human ulnar nerve and observed a pattern of grouped TH-containing axons throughout the fascicles of this nerve. To date, no control data have been provided to account for the problems of nonspecific binding or TH-binding accuracy, and no other mechanism for the disparate results regarding the distributed nature of TH-positive axons can be provided.

The purpose of this study was to examine the distribution of sympathetic C fibers within the human common peroneal nerve (CPN), the nerve most commonly used for human-based sympathetic neural recordings. Second, the study aimed to discuss

Table 1. *Donor information*

Donor No.	Age, yr	Sex	Symptoms at Death
1575	89	Female	Pneumonia, dementia, hypothyroidism, hypertension
1581	71	Male	Pancreatic cancer
1582	90	Female	Bronchopneumonia, Alzheimer's/dementia

how such axonal anatomy relates to recent evidence regarding multiunit action potential recordings and the practice of microneurography. These aims also required that we optimize the immunohistochemical protocol for TH detection in human nerves.

METHODS

Tissue Fixation

Tissue samples were taken from both rats and humans for immunohistochemical staining. Use of cadaveric material for this project received approval through the Internal Research Ethics Committee (Body Bequeathal Programme) within the Department of Anatomy and Cell Biology, The University of Western Ontario, for the extradepartmental use of cadaveric material for research purposes. For the rodent tissues, all procedures complied with the Animal Care guidelines and ethics approval board from The University of Western Ontario.

Rat tissues. Tissues from euthanized Sprague-Dawley rats were used to optimize the TH staining procedure, as well as establish control data. Sciatic nerves were harvested for the purpose of optimizing the TH staining procedure in peripheral axonal tissue. To keep nerve tissue in a reasonable biological length, the ends of the removed sciatic nerves were tied with string and stretched onto a piece of card until nerve bandings disappeared. Adrenal glands and whole brains were excised for use as positive and negative control tissues. Tissues were fixed in formalin for 24 h before being rinsed and stored in 70% ethanol. Finally, tissues were processed overnight (Leica ASP 300) and then embedded in paraffin wax (Thermo Shandon Histocentre 3).

Human tissue. The cadavers were donated to the Bequeathal Program in the Department of Anatomy and Cell Biology at the University of Western Ontario (Table 1). Within 24 h of death, and before embalming, both the right and left CPNs were surgically excised through a 5-cm-long incision over the fibular head of each leg. Indian ink was used to mark the lateral aspect of the nerve, allowing for correct anatomical orientation when the nerve was removed. Each nerve section was fixed to a plastic platform in its in vivo anatomical length. Nerves were then fixed in formalin for 24 h before being rinsed and stored in 70% ethanol. Tissues were processed overnight (Leica ASP 300) and then embedded in paraffin wax (Thermo Shandon Histocentre 3).

Tissue Cutting

Tissue blocks were trimmed of excess paraffin wax and hydrated on ice for at least 30 min. Five-micrometer transverse sections of tissues were made (10 each). In addition, 10-μm longitudinal sections of the human nerves (10 each) were taken to aid in the verification of the sympathetic fiber staining. These slices were placed on a hot water bath before mounting. All slides were incubated overnight at 37°C.

Immunohistochemical Protocol Development

An objective of this investigation was to optimize an immunohistochemical protocol to stain for TH in human tissues. This approach identifies sympathetic C fibers, avoiding detection of sensory C fibers. A major concern was determining the optimal antibody concentration. As human tissues are not always readily available, rat sciatic nerves were used in the protocol development. The protocol outlined here represents the results of the preliminary work performed on rat sciatic nerves.

The ABC immunohistochemical method was used in the present study because of its excellent sensitivity and minimal background staining (12). On the first day, slides were deparaffinized (Leica Auto-stainer XL), submerged in a cartridge of citrate antigen retrieval solution (pH 6.0), placed in a pressure cooker for antigen retrieval at 120°C for 2 h, and then washed in Tween phosphate buffer solution (TPBS) for 5 min. To prevent endogenous peroxidase activity, slides were quenched by placing them in 3% hydrogen peroxide for 15–20 min. During this time, the blocking/avidin solutions were created by mixing 1 ml of 10% goat serum solution with four drops (~180 μl) of avidin (Vector avidin-biotin blocking kit; catalog no. SP-2001). After quenching, slides were washed in TPBS and two changes of phosphate buffer solution (PBS) for 2 min each. Slides were placed in an incubation chamber, and the blocking/avidin solution was applied to each tissue with a 200-μl pipette until there was a dome of solution over the tissue. Lids were placed on the incubation chambers, and slides sat at room temperature for 1–2 h. In the last 15 min of blocking/avidin solution incubation, three different primary antibody solutions (Millipore rabbit polyclonal ant-TH; catalog no. AB152; lot no. NG1723896) were prepared as follows: *1*) negative solution, combined four drops of biotin (Vector avidin-biotin blocking kit; catalog no. SP-2001) to every 1 ml of 1% goat serum solution; *2*) positive solution, combined 1 ml of 1% goat serum solution, four drops of biotin, and anti-TH at a ratio of 1:2,300; *3*) absorbed solution, combined 1 ml of 1% goat serum solution, four drops of biotin, and anti-TH at a ratio of 1:2,300 with 5 μl TH protein (Novus Human TH protein; catalog no. NBP1–43461). Slides were washed for 2 min in PBS before application of these primary antibody solutions. Slides were then individually dried and placed in incubation chambers, and the solution was applied to cover the entire tissue in the same manner as the blocking/avidin solution. Tissues were incubated in the primary antibody solution overnight at room temperature.

Table 2. *Peroneal nerve fascicle characteristics*

Donor No.	Peroneal Nerve CSA, mm^2	No. Fascicles in Section	Total Fascicle CSA, mm^2	Fascicle Size, mm^2			No. Fascicles with SNS Axons	No. Fascicles With/Without TH-positive Axons	Relative CSA of Sympathetic Fascicles, %
				Mean	Median	IQR			
1581-L	12.21	25	1.46	0.061	0.079	0.029	25/25	1	100
1581-R	11.03	27	1.63	0.26	0.075	0.022	26/26	1	100
1582-L	7.21	27	2.05	0.114	0.147	0.049	17/18	0.94	99
1582-R	8.74	27	2.55	0.094	0.127	0.630	26/27	0.96	99
1575-L	12.12	38	0.95	0.032	0.043	0.022	37/38	0.97	99
1575-R	11.31	34	1.24	0.040	0.059	0.020	33/34	0.97	99
AVG	10.44	30	1.65	0.067	0.088	0.034		0.97	99
± SD	2.02	5	0.58	0.031	0.04	0.018		0.02	0.52

Values are from the left (L) and right (R) common peroneal nerves of three individuals. CSA, cross-sectional area of entire nerve (including interfascicle connective tissue); IQR, interquartile range; SNS, sympathetic nervous system; TH, tyrosine hydroxylase. AVG, average of six nerves.
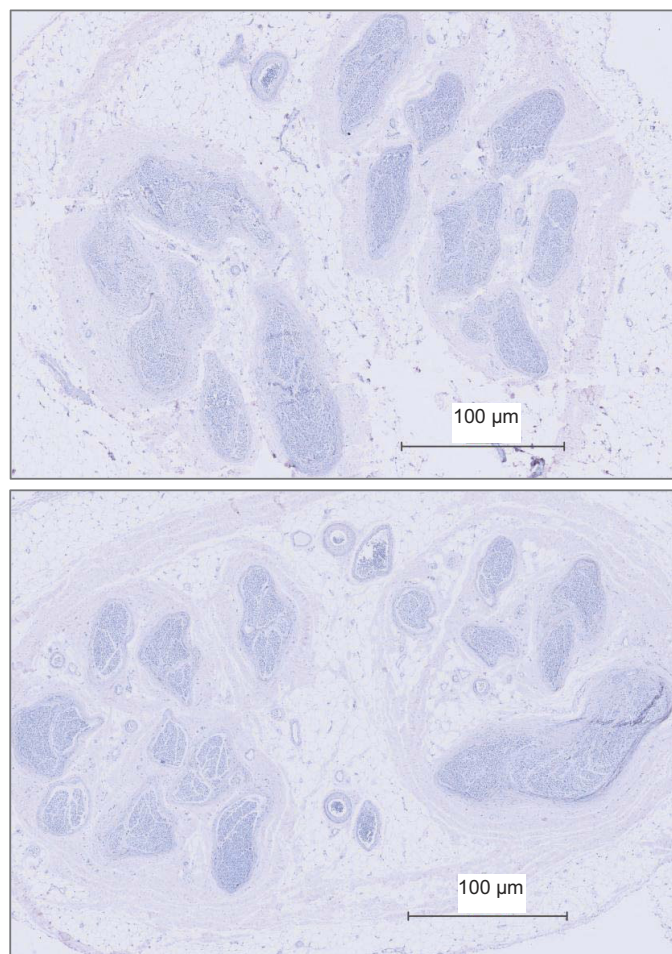
Fig. 1. Fascicle patterns in the right (*top*) and left (*bottom*) common peroneal nerve from *donor 1581*.

On the second day, the 2° antibody solution was prepared by combining biotinylated 2° antibody (Vector Biotinylated anti-rabbit IgG, made in goat; catalog no. BA-1000) and 1% goat serum solution at a ratio of 1:400. Slides were washed in TPBS for 2 min and two changes of PBS for 2 min each. Slides were dried individually, and the 2° antibody was applied to cover the entire tissue. The lids of

incubation chambers were replaced, and tissues were incubated for 1–2 h at room temperature.

While tissues were incubating, the Vectastain Elite ABC reagent was prepared by combining 2.5 ml of PBS with one drop each of *reagents A* and *B*. This solution was prepared at least 30 min before desired application and sat at room temperature for 30 min. When tissue incubation was complete, slides were washed in TPBS for 2 min and two changes of PBS for 2 min each. Individually slides were dried, and Vectastain Elite ABC reagent was applied, covering the entire tissue. Incubation chamber lids were applied, and Vectastain incubation occurred for 1–2 h.

To visualize the locations of the antigen, the peroxidase on the ABC's biotin was developed using 3′3-diaminobenzidine (DAB). DAB will produce a characteristic brown stain where any ABC is found. When incubation was complete, slides were washed in TPBS for 2 min and two changes of PBS for 2 min each. When washing was complete, the DAB solution was prepared by combining 2.5 ml double-distilled water (ddH_2O) with one drop buffer stock, two drops DAB stock, and one drop hydrogen peroxide stock, mixing well between each addition. Individually, slides were dried, and DAB solution was applied to cover entire tissue. Each slide was incubated in DAB for 8 min. After the 8 min, slides were washed using a 1,000-μl pipette with ddH_2O, being careful to avoid placement of ddH_2O directly on the tissue. A total of 5,000 μl were used for each slide. Washed slides were then placed in a Coplin jar of ddH_2O.

Myelin Staining

To verify the location of unmyelinated sympathetic fibers within the whole nerve, eriochrome cyanine R (JT Baker Chemical) was used as a stain for myelin of the other axons. Slides were removed from the ddH_2O and placed into a slide cartridge of eriochrome Cyanine R for 15 min. Slides were then washed with running water to eliminate any unbound stain. To further eliminate staining, leaving only the myelin and erythrocytes stained, slides were differentiated in a 10% aqueous iron aluminum solution for ~20–30 min. Differentiation was complete when staining was removed from background and nuclei. Slides were than washed in running water (13).

Dehydrating and Clearing

Slides were dehydrated and cleared through graded changes of ethanol and xylene (Leica Auto-stainer XL). Slides were then wiped dry, and a coverslip with dinbutyl phthalate in xylene mounting agent was applied. Small concentrations of eosin in the alcohol provided a light counterstain of tissue that was not stained by the immunohistochemistry or eriochrome cyanine R procedures.
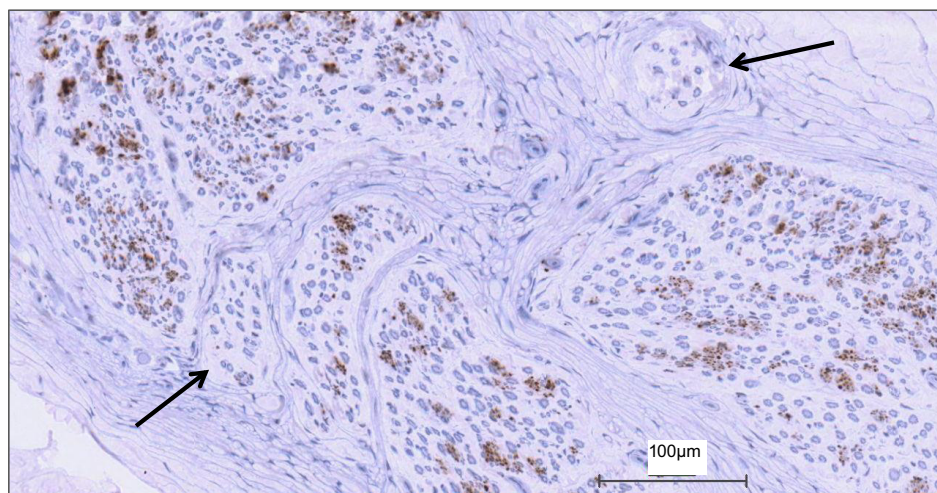

Fig. 2. View of how sympathetic fibers (positively stained for tyrosine hydroxylase) vary with each fascicle in a representative section of the common peroneal nerve. The amount of staining within a fascicle varied between fascicles of the same nerve. Some fascicles displayed no staining, while others showed a large abundance. Black arrows indicate fascicles with no sympathetic axons.

Table 3. *Characteristics of TH-positive axons in the common peroneal nerve*

Donor No.	No. Axons Total	Axons/Fascicle			Axon Density, per mm^2		
		Mean	Median	IQR	Mean	Median	IQR
1581-L	8,951	358	476	180	9,197	9,704	3,614
1581-R	18,549	713	1,060	552	19,954	14,131	4,274
1582-L	5,081	181	432	230	3,710	4,621	1,602
1582-R	2,901	107	139	61	1,583	2,082	1,072
1575-L	5,124	165	197	70	8,772	12,046	4,525
1575-R	4,272	126	170	62	5,428	7,062	3,674
AVG	7,480	275	412	193	8,107	8,274	3,127
± SD	5,784	232	247	190	6,497	4,555	1,439

Values are from the L and R common peroneal nerves of three individuals.

Control Tissues

Negative control tissues. To examine secondary binding characteristics, two negative controls were used for each tissue, with the expectation of minimal staining after the DAB visualization step. These controls included *1*) the omission of primary antibody, and *2*) an absorption control (2, 3).

Positive control tissues. To determine accuracy of antibody binding (22), the TH immunohistochemistry procedure was performed on rat adrenal gland medulla and corpus striatum, tissues that demonstrate intense and distinctive patterns of TH distribution. As a further verification that actual sympathetic nerve axons were being stained, the TH staining procedure was repeated on the longitudinal nerve sections of the human peroneal nerve.

Viewing and Imaging Slides

Slides were viewed with a standard light microscope through ×5, ×10, ×40, and ×100 objectives. Two methods were used to photograph the nerves. First, three of the superior quality slides, from *donor 1581*, were digitized using Aperio slide digitizer and software: a right and left CPN, and a right CPN with an absorbed control. The remaining slides were photographed using a Zeiss Axiovert 200 inverted microscope and Axio HRc camera. Only select slides and regions were photographed, as it was not possible to image the entire nerve section at higher magnifications.

Fascicle and Axon Characteristics

The numbers and cross-sectional area (CSA) of fascicles were quantified at ×10–20 magnification, and their CSAs (excluding perineurium), together with the CSA of the whole nerve, were determined using ImageJ software. The mean, median, and interquartile range of fascicular CSAs, and whether or not they contained TH-positive axons, were quantified.

Under ×40–100 magnification, TH-stained axons were counted manually within each fascicle with emphasis on whether they were viewed as single axons or in bundles. The nature of bundled groupings was subjective and based on whether or not all axons in a bundle possibly would be interrogated by a single electrode position. The number of axons, axonal density, and distribution data of mean, median, and interquartile range of bundles within each fascicle were calculated.

RESULTS

Fascicle Number and Size

The CPN CSA at the fibular head site was 10 ± 2 mm^2 (Table 2) of which ~20% was occupied by fascicles (excluding perineurium). Total nerve fascicle number ranged from 25 to 38 (Table 2). The fascicle number was typically consistent across the various slices from the same nerve (data not shown), but not between individuals (Table 2; Fig. 1). Specifically, differences in right vs. left fascicular number ranged from 12 in *donor 1581* to 7–8 in *donor 1582*. Of the six collected nerves, fascicle number could not be calculated accurately for the left nerve of *donor 1575* due to damage to the anterior region of the nerve section during the staining procedure. Also, fascicular number will be affected by the stage of branching in the specific section. In some cases, distinct intrafascicular divisions were evident, separated by what appeared to be perineurium. In this case, such divisions were counted as separate fascicles. Fascicle size was noticeably variable, both within, and between, individuals (Table 2). Both left and right nerves of *donor 1575* had numerous small fascicles, and *donor 1582* displayed a smaller number of large fascicles. Less than 1% of the nerve fascicles contained no TH-stained axons (Table 2). These fascicles tended to be smaller in size (Fig. 2).

Table 4. *Bundled characteristics of TH-positive axons in the common peroneal nerve*

Donor No.	No. Bundles Total	Bundles/Fascicle			Axons/Bundle					1-Fiber Bundles, %
		Mean	Median	IQR	Mean	Median	IQR	Max	Min	
1581-L	2,265	91	124	50	4.38	5.70	1.52	41	1	36
1581-R	4,320	166	216	87	4.67	6.24	2.75	44	1	9
1582-L	1,622	95	148	85	3.13	3.76	1.02	44	1	21
1582-R	1,180	45	49	22	3.03	3.82	1.21	42	1	16
1575-L	1,818	49	69	30	3.48	4.26	0.96	39	1	18
1575-R	1,392	42	50	21	3.13	3.86	0.82	39	1	15
AVG	2100	81	109	49	4	5	1	42	1	19
± SD	1150	48	66	30	1	1	1	2	0	9

Values are from the L and R common peroneal nerves of three individuals. Bundles include those containing 1−44 axons, but the proportion of those with only 1 axon are indicated in the right column.
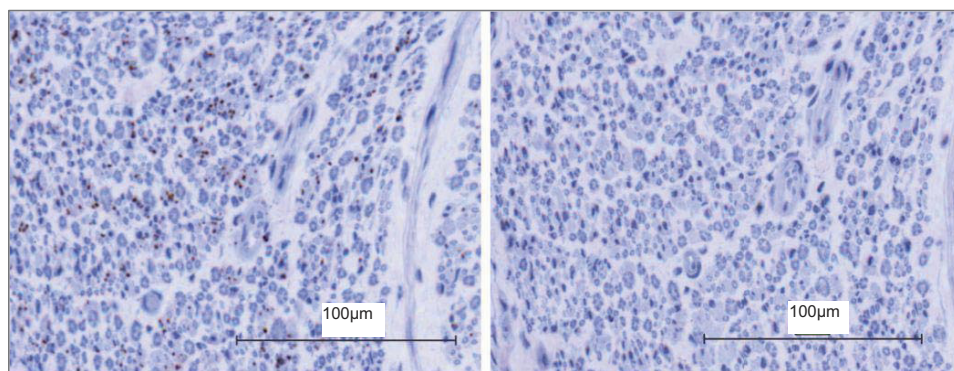
Fig. 3. Individual sympathetic fiber arrangement within the human common peroneal nerve. *Left*: positively stained nerve; sympathetic fibers are illustrated as brown dots between the blue stained myelinated fibers. *Right*: negative control nerve section.

Sympathetic Fiber Arrangement and Size

The quantitative details regarding axonal characteristics are provided for each individual in Tables 3 and 4. It is important to note that the axonal count data should be viewed as an estimate, because variations in staining intensity, and the tightly-packed nature of C-fibers in bundles, generated difficulty in differentiating individual axons. Within this constraint, it was estimated that the content of TH-positive axons ranged from 2,901 to 18,549 across the individual nerves, with a fascicular density of 2,082–14,131 axons/mm^2 (Table 3). One interesting observation was the threefold greater number of sympathetic C fibers in the left vs. right CPN of *donor 1581*, despite similar overall nerve CSA and fascicle number.

Within fascicles that did express TH-positive staining, some fibers existed as individual axons (Fig. 3), but most were grouped in bundles (Fig. 4). As shown in Table 4, ~275 ± 233 bundles/fascicle were observed, and these ranged in size from 1 to 42 ± 2 axons/bundle. However, the distribution of bundle size was highly skewed toward smaller bundles, with the median value of 5 axons/bundle (interquartile range of 1; Table 4). Approximately 20% of the axonal "bundles" existed as single

neurons. There seemed to be no pattern between fascicle size and sympathetic fiber concentration between the left and right nerves from the same donor, or within a single nerve section. Furthermore, in the current visual analysis of a limited number of nerves, no particular pattern could be observed regarding the location of individual or grouped TH-containing axons (Fig. 5). Diameter of the TH-containing axons ranged from approximately <1 to 2 μm; these are viewed best in Figs. 6 and 9.

Although the axon and bundle counts are considered to be estimates, the consistency of measurement was supported by the repeated assessment of axon arrangement in the right nerve of *donor 1575* on separate days separated by 1 wk. The linear regression results are as follows: for axons/fascicle, $r = 0.96$, slope $= 1.01$, $P < 0.0001$; for the number of axonal bundles/fascicle, $r = 0.99$, slope $= 0.94$, $P < 0.0001$; for individual neurons, $r = 0.97$, slope $= 0.97$, $P < 0.0001$; for the median bundle size, $r = 0.89$, slope $= 0.75$, $P < 0.0001$.

Control Measures

Longitudinal nerve sections produced TH-positive staining along the length of the nerve segment (Fig. 6). Rat adrenal
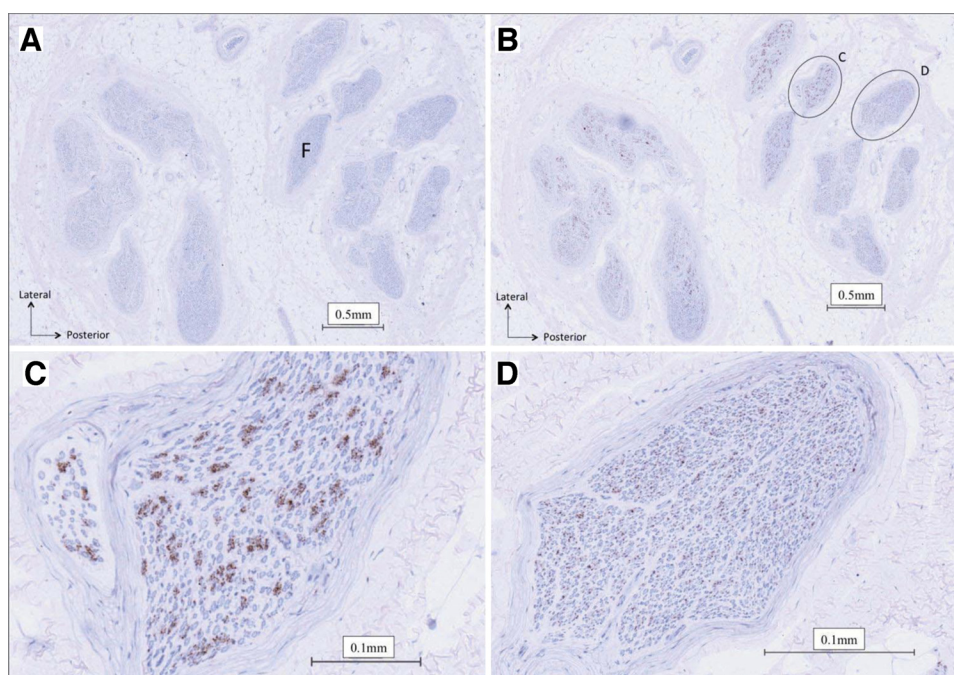

Fig. 4. Cross section of right human common peroneal nerve. *A*: nerve section used as a negative control. *B*: positively stained nerve section. Sympathetic axons are represented by brown regions within the nerve fascicles (F). Myelinated fibers are represented by the blue circles in the fascicle. *C* and *D*: enlargements from *B* of a positively stained nerve fascicles demonstrating the differences in arrangement between fascicles.

Fig. 5. Sympathetic axon arrangement in right and left common peroneal nerve of *donor 1581*. A: right common peroneal nerve section used as a negative control. B: positively stained right common peroneal nerve. C: left common peroneal nerve section used as a negative control. D: positively stained left common peroneal nerve.
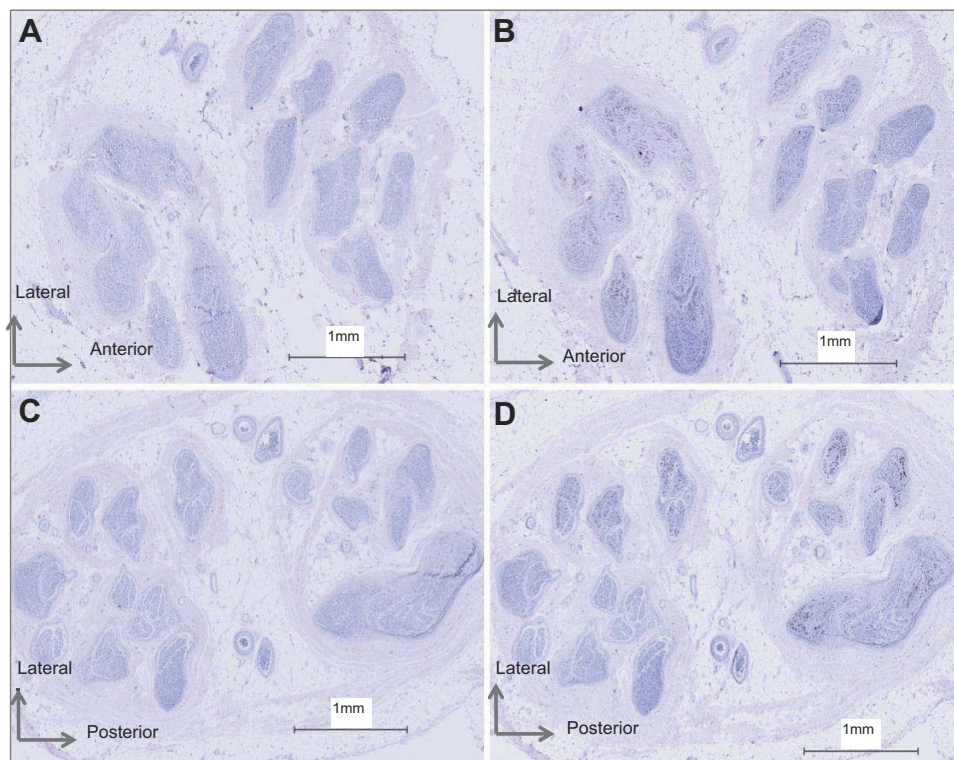
gland and striatum cortex each produced significant TH staining (Figs. 7 and 8), exhibiting the accuracy of the TH staining procedure. Of interest, however, was the observation that, while the majority of staining in the adrenal gland was localized to the medulla, some also extended into the adrenal cortex, a region devoid of norepinephrine production (Fig. 7). The two negative control experiments performed on the human nerve with no primary antibody (Figs. 4 and 5) and human nerve with absorbed antibody serum (Fig. 9) each demonstrated no TH-containing axons.

DISCUSSION

The main observation from this study was that sympathetic axons within the human CPN can exist as single axons but generally are grouped in bundles of 2–42 axons with unpredictable scattering. These bundles were present in most, but not all, fascicles.

Immunohistochemistry Details

An important difference between this study and earlier work (1, 19, 21) was the primary antibody dose. It was essential that only the sympathetic fibers stained positively with DAB. Thus, in preliminary work, varying concentrations of 1° antibody were tested, which revealed that the concentration of 1:2,300 (0.5 μl of 1° antibody for 1,180 μl) optimized the sympathetic fiber resolution. Previously, higher concentrations of 1:200 and 1:1,000 were used (1, 19, 21), but these earlier studies provided inconsistent sympathetic fiber patterns. In addition, staining for surrounding tissues such as myelin sheath enhanced differentiation of C fibers from the myelinated fibers. This process exposed these tissue types and verified that the sympathetic fibers were not myelinated.

The specificity of TH-containing axons in the peroneal nerve was verified by the TH-negative control studies and also the TH-positive control studies performed in the rodent adrenal

Fig. 6. Longitudinal sections of sympathetic axons from the human common peroneal nerve. *Left*: positively stained fibers can be seen traveling along the length of nerve. *Right*: negative control longitudinal section.
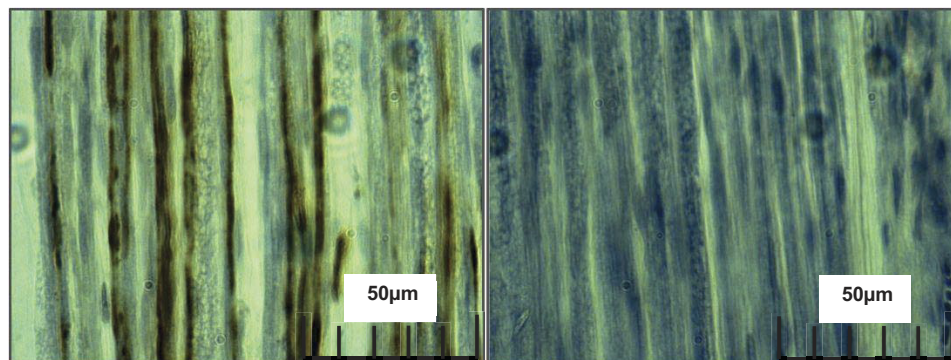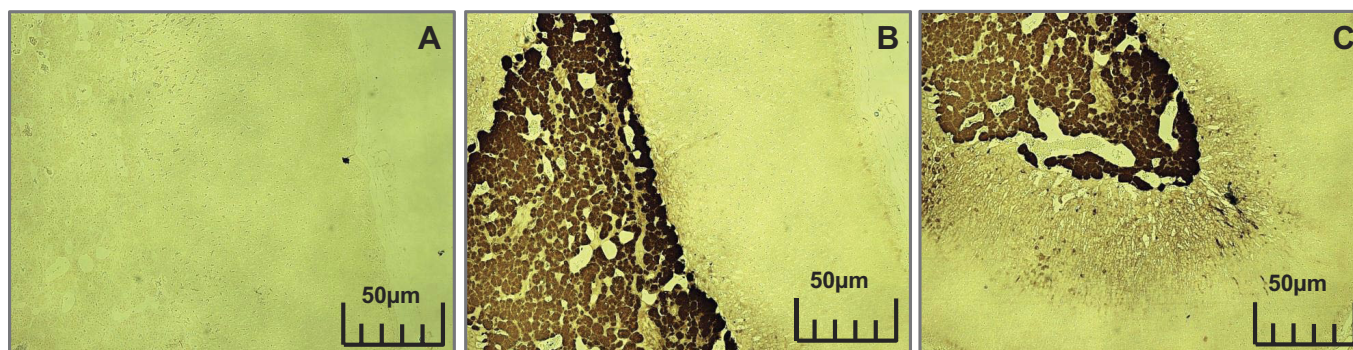
Fig. 7. The adrenal medulla from rat with tyrosine hydroxylase staining. *A*: adrenal medulla used as a negative control. *B*: positively stained adrenal medulla. *C*: positive staining in the adrenal cortex.

medulla and corpus striatum tissues. However, regions of the adrenal cortex adjacent to the medulla also stained positively for TH, even though norepinephrine biosynthesis does not occur in this tissue. The reasons for this staining pattern are unknown. The TH-positive staining of selective axons in the longitudinal nerve slices provide further verification that the positive TH staining in the nerve cross-section slices were true axons.

General Anatomical Considerations

As expected (4, 18), fascicle number and size varied between nerves from the same donor and between donors. These observations indicate that fascicle number seems to change over very short distances in peripheral nerves (20), likely demonstrating the branching of peripheral nerves to innervate passing structures.

Within each fascicle, the sympathetic fibers were arranged in two general patterns, namely as individual axons and in bundles. By visual inspection of distinct single TH-containing fibers, the diameter of these C fibers ranged from ~0.5 to 2.0 µm and often 1 µm or less. These dimensions are in general agreement with electron microscopy studies of all-type unmyelinated fibers in the sciatic nerves of mice (8) and rats (11, 26). Analysis of diameter distributions of unmyelinated axons from the rat sciatic nerve before and following sympathectomy suggests that sympathetic fibers are generally 0.5–1.2 µm (27).

Our evidence that most, but not all, fascicles contained TH-positive axons confirm the patterns identified earlier (1) in the forearm nerves and extend them to the CPN of humans.

The current analysis has emphasized the bundled nature of TH-positive axons in the CPN. The exact number of axons in each bundle was difficult to establish in this immunohistochemical approach, because overlap of staining appeared to occur between some juxtaposed axons. Nonetheless, this analysis suggests that the largest sympathetic bundles contained up to ~44 axons in the nerve sample. This number of axons/bundle fits well with recent microneurographic analysis of axonal content within multiunit bursts of efferent postganglionic sympathetic nerve activity (24, 28), where a maximum of 40 action potentials were observed during very strong chemoreflex or baroreflex stress. Certainly, we suspect that some of these action potentials were due to repetitive firing of the same axon within the same burst (15, 16). However, the probability data indicate that most axons fire only once per cardiac cycle (15, 16). Therefore, the current analysis provides an anatomical basis for understanding the maximal limit of action potentials within a given burst of sympathetic nerve activity. This number will depend upon the particular bundle of sympathetic fibers impaled by the microelectrode. Moreover, the current evidence enables construction of a clearer picture regarding the practice of microneurography and the relationship between microneurographic electrode position and record-
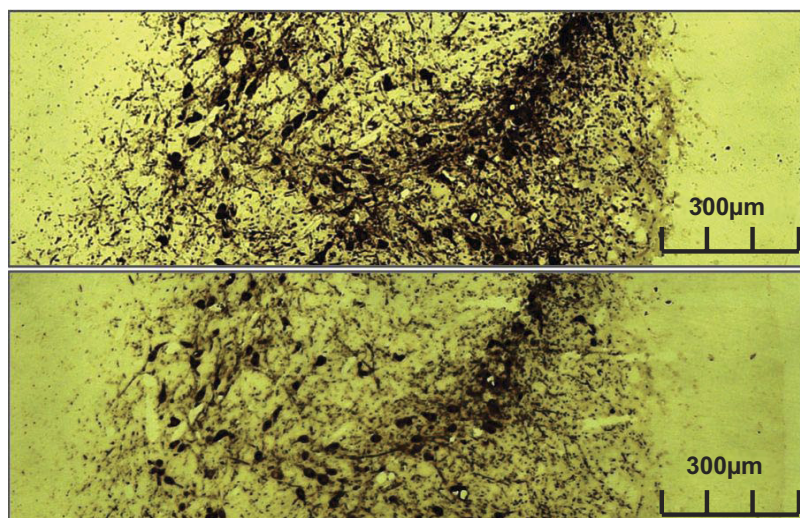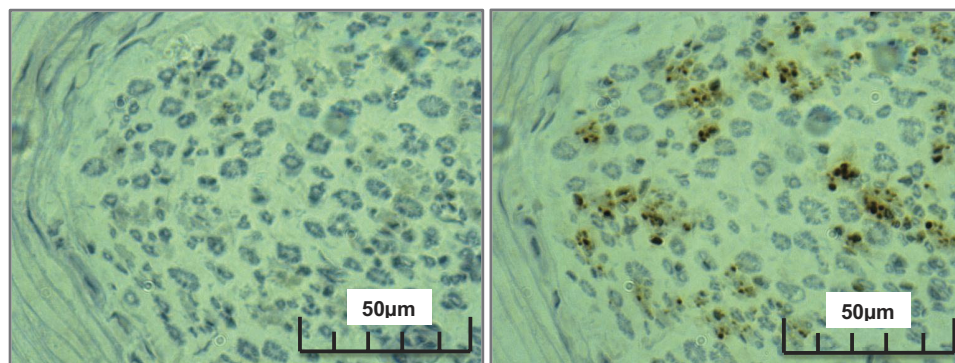

Fig. 8. Rat corpus striatum used as a positive control. *Top*: positively stained rat brain. *Bottom*: rat brain with absorbed serum.

Fig. 9. Absorbed control on left human common peroneal nerve. *Left*: absorbed anti-tyrosine hydroxylase serum control. *Right*: positively stained nerve section.

ing success. To enhance this illustration, a schematic microelectrode of characteristic dimensions (200 μm shaft, 5 μm tip) has been overlaid onto one of the cross-sectional images from the current study (Fig. 10). This picture highlights the anecdotal experience of this technique that *1*) some parts of the nerve contain higher density of active recording sites than others; and *2*) electrode position can provide small or large bursts with very small adjustments.

Another anecdotal experience of microneurographers is that high-quality muscle sympathetic nerve recordings are obtained easily in some individuals, but not in others, although the baseline burst rates are highly reproducible, regardless of the recording quality (7, 14). The current anatomical data may explain these observations. First, most bundles are probably too small to give an adequate reporting of a "burst" in the

integrated neurogram. This determination comes from our laboratory's previous observations of action potential recruitment patterns in the CPN, which indicate the smallest detectable burst in the integrated neurogram (using a signal-to-noise ratio of >3) requires approximately four or more axons to be recruited synchronously (24, 28). The majority of bundles appear to be in this range, or smaller. However, while each nerve expressed fascicles with large bundles (Table 4), there are a greater number of larger bundles in some individuals than in others, enhancing the probability of successful and higher quality recordings in only a subset of a group. The reproducibility of burst frequency noted above would merely require that the microelectrode interrogate any bundle of sufficient size to produce sufficient (e.g., 4 or more) axons firing at the same time.
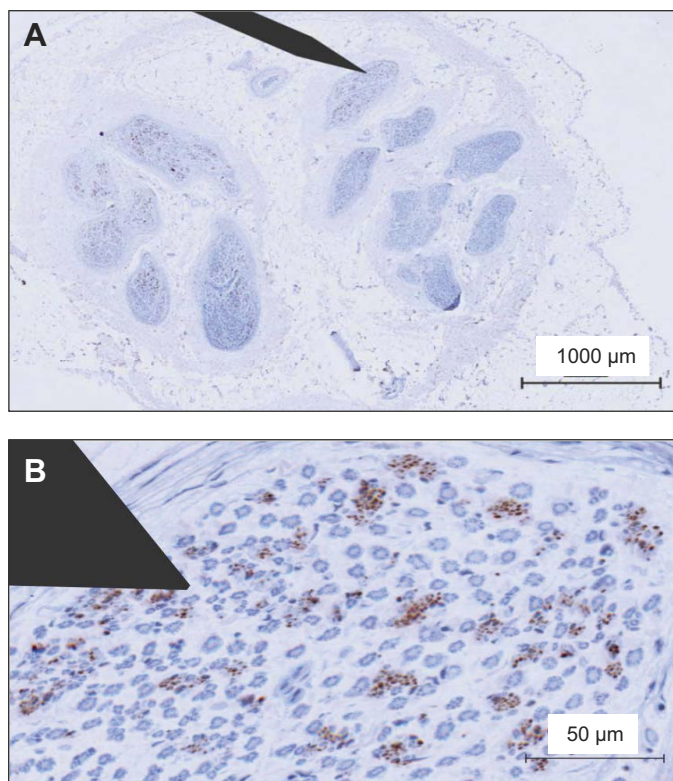
Limitations

No published literature exists regarding human TH half-life. The rat unphosphorylated TH has a half-life of 15 min at 50°C, requiring harvesting of tissue as soon as possible postmortem (9). Previous studies on cadaver nerves suggest removal of tissue within 6–10 h after death (20, 21). In the present study, tissue extraction occurred within 24 h of death, but not before 6 h. Thus TH breakdown must have occurred in our cadaver tissues with the probable consequence of diminishing the staining density. Regardless, the specificity of TH staining in the rat tissues (harvested within minutes of rodent death), and the consistent staining of TH in cross-sectional, and longitudinal, slices support the conclusions that the staining patterns within the human nerves reflected TH-containing axons.

Second, not all TH-containing axons will reflect the same "type" of sympathetic C fiber. Some of these will contain axons directed to targets in the skin, whereas others will be directed toward the vasculature within skeletal muscle. No determination of such targeting can be made from the current observations.

The small sample size provides a third limitation. Nonetheless, the general pattern of axonal groupings was consistent across all six nerves. Finally, these nerve segments were obtained from elderly individuals who suffered from various diseases at the time of death. The impact of age and disease on efferent sympathetic nerve activity is well described, but whether such changes are accompanied by altered ultrastructural changes in C-fiber axonal expression are not known.

Fig. 10. Schematic of microneurographic microelectrode overlaid on a common peroneal nerve slice (*A*) with enlarged image (*B*) to illustrate relationship between microelectrode and sympathetic axon bundles in this nerve.

AUTHOR CONTRIBUTIONS

Author contributions: R.P.T. and C.M. performed experiments; R.P.T., T.D.W., and B.D.B. analyzed data; R.P.T. and T.D.W. prepared figures; R.P.T. drafted manuscript; R.P.T., C.M., T.D.W., B.D.B., and J.K.S. approved final version of manuscript; C.M. and J.K.S. interpreted results of experiments; C.M., T.D.W., and J.K.S. edited and revised manuscript; J.K.S. conception and design of research.

REFERENCES

1. **Balogh B, Valencak J, Vesely M, Flammer M, Gruber H, Piza-Katzer H.** The nerve of Henle: an anatomic and immunohistochemical study. *J Hand Surg Am* 24: 1103–1108, 1999.
2. **Bancroft JD, Gamble M.** *Theory and Practice of Histological Techniques.* Edinburgh, UK: Churchill Livingstone Elsevier, 2008.
3. **Burry RW.** Controls for immunocytochemistry: an update. *J Histochem Cytochem* 59: 6–12, 2011.
4. **Captier G, Canovas F, Bonnel F, Seignarbieux F.** Organization and microscopic anatomy of the adult human facial nerve: anatomical and histological basis for surgery. *Plast Reconstr Surg* 115: 1457–1465, 2005.
5. **Dellon AL, Hoke A, Williams EH, Williams CG, Zhang Z, Rosson GD.** The sympathetic innervation of the human foot. *Plast Reconstr Surg* 129: 905–909, 2012.
6. **Diedrich A, Charoensuk W, Brychta RJ, Ertl AC, Shiavi R.** Analysis of raw microneurographic recordings based on wavelet de-noising technique and classification algorithm: Wavelet analysis in microneurography. *IEEE Trans Biomed Eng* 50: 41–50, 2003.
7. **Fagius J, Wallin BG.** Long-term variability and reproducibility of resting human muscle nerve sympathetic activity at rest, as reassessed after a decade. *Clin Auton Res* 3: 201–205, 1993.
8. **Fazan VP, Ma X, Chapleau MW, Barreira AA.** Qualitative and quantitative morphology of renal nerves in C57BL/6J mice. *Anat Rec* 268: 399–404, 2002.
9. **Gahn LG, Roskoski R Jr.** Thermal stability and CD analysis of rat tyrosine hydroxylase. *Biochemistry* 34: 252–256, 1995.
10. **Hagbarth KE, Vallbo AB.** Pulse and respiratory grouping of sympathetic impulses in human sympathetic nerves. *Acta Physiol Scand* 74: 96–108, 1968.
11. **Hanada T, Uchida S, Hotta H, Aikawa Y.** Number, size, conduction, and vasoconstrictor ability of unmyelinated fibers of the ovarian nerve in adult and aged rats. *Auton Neurosci* 164: 6–12, 2011.
12. **Hsu SM, Raine L.** Protein A, avidin, and biotin in immunohistochemistry. *J Histochem Cytochem* 29: 1349–1353, 1981.
13. **Kiernan JA.** *HIstological and Histochemical Methods: Theory and Practice.* Oxfordshire, UK: Scion, 2008.
14. **Kimmerly DS, O'Leary DD, Shoemaker JK.** Test-retest repeatability of muscle sympathetic nerve activity: influence of data analysis and head-up tilt. *Auton Neurosci* 114: 61–71, 2004.
15. **Macefield VG, Wallin BG.** Firing properties of single vasoconstrictor neurones in human subjects with high levels of muscle sympathetic activity. *J Physiol* 516: 293–301, 1999.
16. **Macefield VG, Wallin BG, Vallbo AB.** The discharge behaviour of single vasoconstrictor motoneurones in human muscle nerves. *J Physiol* 481: 799–809, 1994.
17. **Marx SC, Dhalapathy S, Marx CA, Babu MS, Pulakunta T, Vasanthakumar.** Ultrasonographical and histological cross-sectional study of the human superficial branch of the radial nerve. *Rom J Morphol Embryol* 52: 1081–1090, 2011.
18. **Marx SC, Kumar P, Dhalapathy S, Anitha MC.** A comparative microanatomical study on cross sections of medial and lateral cutaneous nerves of forearm at the antecubital fossa: a cadaveric study. *Ann Anat* 192: 107–115, 2010.
19. **Marx SC, Kumar P, Dhalapathy S, Marx CA, D'Souza AS.** Distribution of sympathetic fiber areas of radial nerve in the forearm: an immunohistochemical study in cadavers. *Surg Radiol Anat* 32: 865–871, 2010.
20. **Marx SC, Kumar P, Dhalapathy S, Prasad K, Marx CA.** Microanatomical and immunohistochemical study of the human radial nerve at the antecubital fossa. *Ann Anat* 191: 389–398, 2009.
21. **Marx SC, Kumar P, Dhalapathy S, Prasad K, Marx CA.** Microanatomical and immunohistochemical study of the human lateral antebrachial cutaneous nerve of forearm at the antecubital fossa and its clinical implications. *Clin Anat* 23: 693–701, 2010.
22. **Polak JM, Van Noorden S.** *Introduction to Immunocytochemistry.* Oxford, UK: Bios Scientific, 1997.
23. **Salmanpour A, Brown LJ, Shoemaker JK.** Spike detection in human muscle sympathetic nerve activity using a matched wavelet approach. *J Neurosci Methods* 193: 343–355, 2010.
24. **Salmanpour A, Brown LJ, Steinback CD, Usselman CW, Goswami R, Shoemaker JK.** Relationship between size and latency of action potentials in human muscle sympathetic nerve activity. *J Neurophysiol* 105: 2830–2842, 2011.
25. **Salmanpour A, Shoemaker JK.** Baroreflex mechanisms regulating the occurrence of neural spikes in human muscle sympathetic nerve activity. *J Neurophysiol* 107: 3409–3416, 2012.
26. **Sato KL, do Carmo JM, Fazan VP.** Ultrastructural anatomy of the renal nerves in rats. *Brain Res* 1119: 94–100, 2006.
27. **Schmalbruch H.** Fiber composition of the rat sciatic nerve. *Anat Rec* 215: 71–81, 1986.
28. **Steinback CD, Salmanpour A, Breskovic T, Dujic Z, Shoemaker JK.** Sympathetic neural activation: an ordered affair. *J Physiol* 588: 4825–4836, 2010.
29. **Tan CO, Taylor JA, Ler AS, Cohen MA.** Detection of multifiber neuronal firings: a mixture separation model applied to sympathetic recordings. *IEEE Trans Biomed Eng* 56: 147–158, 2009.